2P6-4

Proceedings of Symposium on Ultrasonic Electronics, Vol. 36 (2015)
5-7 November, 2015

Performance Analysis of MC-MFSK Communication System over Multipath Fading Underwater Channel

Dandan Xue†, Jihyun Park, Minja Bae, Jongju Kim, Kyu-Chil Park and Jong Rak Yoon
(Dept. of Inf. and Comm. Eng., Pukyong National Univ., Korea)

1. Introduction

In underwater acoustic communication system, multipath propagation is an important consideration, particularly in shallow water environments. Firstly, the multipath delay spread causes inter-symbol interference (ISI) if the symbol rate increases for high speed communication. Secondly, the transmitter or receiver motion and sea surface fluctuations can result in the center frequency of the signal varied to its left or right side, which is often called Doppler spread in communication which can lead to incorrect symbol decoding, especially in non-coherent demodulation[1,2]. Thirdly, multipath fading can make the signal amplitude destructively or constructively fluctuated and relative phase of the signal frequencies to fluctuate non-linearly, this will result in signal spectrum fluctuation[3].

This paper addresses how the time-varying underwater acoustic multipath fading channel affects the BER of MC-MFSK system. The channel characteristics such as channel impulse response, channel coherence bandwidths and fading statistics, error frequency distributions are related to bit error rate (BER).

2. Experiment

The experiment was conducted in about 20 m depth ocean near Geoje island in Korea on Aug. 6, 2014. The experimental configuration and parameters are shown in **Fig. 1** and **Table I**.

Four channel 4FSK (4C-4FSK) which has a total of 16 frequencies. The orthogonal frequency spacing is given by 1/T (T: symbol period). Frequency guard-band between channels is inserted by 1/T to reduce inter carrier interference.

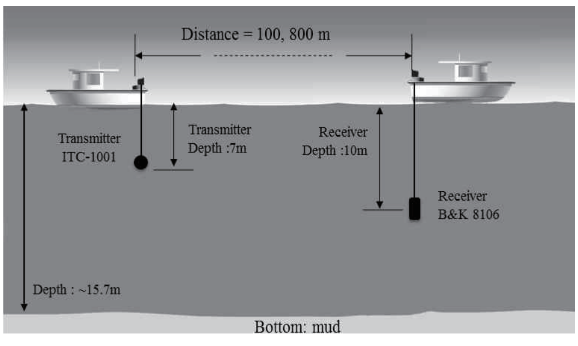

Fig. 1 Experimental configuration.

Table I. Experimental parameters.

Modulation	4C-4FSK
Depth(m)	~15.7
Data rate(bps)	200,400,800,1600
Carrier frequency(kHz)	12-19.2
Tx-Rx Distance(m)	100,800
Tx and Rx depth(m)	7,10
Bottom property	Mud
Information data(bit)	20,000

Figure 2 shows a frame structure of a signal. Each frame lasts 1 s. A linear frequency modulated (LFM) signal of 12 to 18 kHz bandwidth was used for the purpose of measuring the channel response. PN signal of 13 to 19 kHz bandwidth was used for symbol synchronization. In actual system, only one of LFM or PN signals can be used for channel impulse response and symbol synchronization and then the payload can be increased.

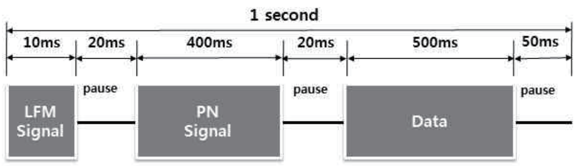

Fig.2 Frame structure.

Figure 3 shows the eigenray trace results. In Fig.3, a numerical value of each eigenray means grazing angle with respect to sea surface plane and only the first five arrivals are shown.

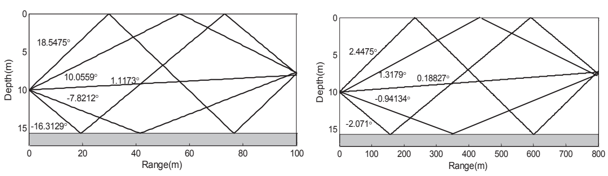

(a) (b)

Fig. 3 Simulated eigenray trace results of four different Tx-Rx ranges: transmitter depth 7 m, and receiver depth 10 m: (a) 100 m; (b) 800 m.

3. Results

The channel impulse response was analyzed by multipath intensity profile (MIP) which is given by matched filtering the received LFM signal with the transmitted signal. **Fig. 4** shows the MIPs of 100 and 800 m Tx-Rx ranges. The first strong signals are pretty stable at both two ranges. The surface reflected signals are also clear in both two

xuedan01@outlook.com

ranges but in 800m range it is almost lumped together with the direct signal.

Fourier-transformed spectra of average signals of 10s MIPs in **Fig. 4** are shown in **Fig. 5**. The coherence bandwidths of -3dB at 100 and 800m ranges are about 60 and 200Hz, respectively. The signal bandwidth of 4FSK is about one fourth of data rate (bps). Therefore only 200 bps at 100m range satisfies a frequency non selective channel. However, 200, 400 and 800 bps at 800 m range satisfy a frequency non selective channel.

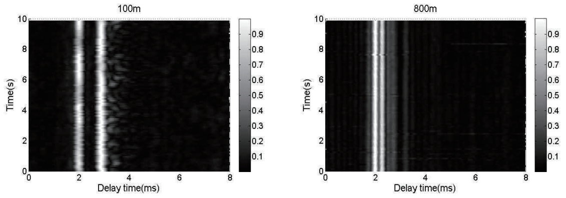

(a) (b)

Fig. 4 Measured channel impulse responses as a function of the delay time and geo-time: (a) 100 m; (b) 800 m.

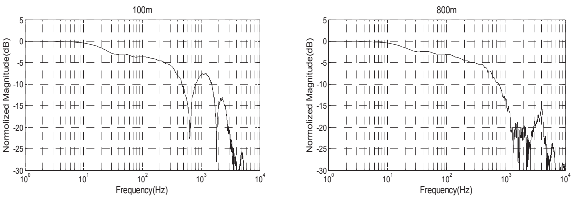

(a) (b)

Fig. 5 Channel coherence bandwidths for four Tx-Rx ranges: (a) 100 m; (b) 800 m.

Table II shows the received images and BERs of four different data rates at 100 and 800m Tx-Rx ranges. At the 100 m range, even the 200bps which satisfies a frequency non selective channel shows BER of 0.007 and BER changes non-linearly. At the 800 m range, there are not any errors in 200 and 400 bps which satisfy a frequency non selective channel and BERs of other data rate changes non-linearly. The data rate changes actually the orthogonal carrier frequency set of 4FSK.

Table II. Received images and BERs.

	200 bps	400 bps	800 bps	1600 bps
100 m				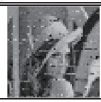
BER	0.007	0.007	0.027	0.043
800 m				
BER	0	0	0.021	0.029

Figure 6 shows error distributions of 4C-4FSK for 1600 bps as a function of carrier frequency and geo-time for 100 and 800 m Tx-Rx ranges. In 100 m range, the errors mainly occur in 16.8 kHz frequency of Ch3 and 18 kHz and 19.2 kHz of Ch4. In 800 m range the errors only occur in Ch2 and Ch4. Therefore, the error of MC-MFSK system closely bounds up with a carrier frequency dependent multipath fading which may result in a frequency dependent signal-to-noise ratio (SNR) fluctuation. The analysis of non-linearity of BER is ongoing as a function carrier frequency set, Tx-Rx range and a multipath fading statistics.

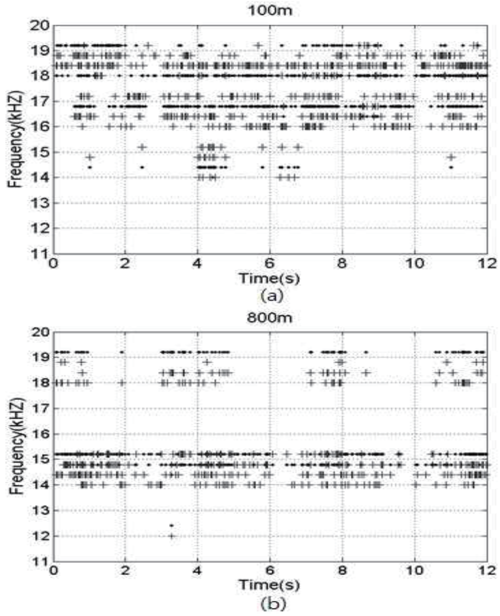

Fig. 6 Error distributions of 4C-4FSK signals based on frequency and geo-time: (a) 100 m; (b) 800 m (. is original frequency; + is error frequency).

4. Conclusions

The BERs of 4C-4FSK system for four different data rates are examined for four Tx-Rx ranges. The BER of a different data rate or different Tx-Rx range depends on not only the channel coherent bandwidth but also the orthogonal carrier frequency set of 4FSK.

Acknowledgment

This research was supported by the 'ISABU Creative Research Program (PE99361)' of the Korea Institute of Ocean Science & Technology (KIOST).

References

1. R. M. Heitsenrether and M. Badiey: AIP Conf. Proc. **728** (2004) 214.
2. A. Falahati, B. Woodward, and S. C. Bateman: IEEE J. Oceanic Eng. **16** (1991) 12.
3. J. Park, C. Seo, K. Park, and J. R. Yoon: Jpn. J. Appl. Phys. 50 (2013) 07HG01.